

# Modelling recombinations during cosmological reionization

Milan Raičević<sup>1,2\*</sup> and Tom Theuns<sup>1,3</sup>

<sup>1</sup>*Institute for Computational Cosmology, Durham University, Science Laboratories, Durham DH1 3LE, UK*

<sup>2</sup>*Leiden Observatory, Leiden University, P.O. Box 9513, 2300RA Leiden, The Netherlands*

<sup>3</sup>*Universiteit Antwerpen, Campus Groenenborger, Groenenborgerlaan 171, B-2020 Antwerpen, Belgium*

## ABSTRACT

An ionization front expanding into a neutral medium can be slowed-down significantly by recombinations. In cosmological numerical simulations the recombination rate is often computed using a ‘clumping factor’ that takes into account that not all scales in the simulated density field are resolved. Here we demonstrate that using a single value of the clumping factor significantly overestimates the recombination rate, and how a local estimate of the clumping factor is both easy to compute, and gives significantly better numerical convergence. We argue that this lower value of the recombination rate is more relevant during the reionization process and hence that the importance of recombinations during reionization has been overestimated.

**Key words:** radiative transfer – methods:numerical – cosmology: dark ages, reionization, first stars

## 1 INTRODUCTION

The intergalactic medium is highly ionized by the UV-background produced by QSOs and galaxies, at least since  $z \sim 6$  (Gunn & Peterson 1965; Haardt & Madau 1996; Rauch 1998). Reionization – the transition from neutral to ionized – occurred around  $z_{\text{reion}} \sim 10$ , according to the Thomson optical depth inferred from the cosmic-microwave background (see Komatsu et al. 2010, for 7-year WMAP result). Reionization starts when the first sources of ionizing photons form small, isolated HII regions around them. As more and increasingly luminous sources form, ionized regions become larger and more numerous, until they eventually percolate space, signalling the end of the epoch of reionization (EoR, Arons & Wingert 1972; Haardt & Madau 1996; Giroux & Shapiro 1996; Gnedin & Ostriker 1997; Haiman & Loeb 1997, see recent reviews by *e.g.* Barkana & Loeb 2001; Ciardi & Ferrara 2005; Loeb 2006).

The nature of the sources of ionizing photons is currently unknown, with ‘first stars’, early galaxies, and black hole accretion, probably all contributing to some extent (*e.g.* Madau et al. 1999). We recently demonstrated that the early population of galaxies predicted by Durham’s GALFORM model produce enough ionizing photons to complete reionization by  $z \sim 10$  (Raičević et al. 2010a). The same model also matches very well the luminosity function of redshift  $z = 7 - 10$  galaxies recently discovered by the *Hubble Space Telescope* (Bouwens et al. 2008; Bouwens et al.

2009). In this model, the bulk of photons are produced in low-mass ( $M_{\star} \sim 10^6 h^{-1} M_{\odot}$ ), gas-rich, faint galaxies (rest-frame UV magnitude  $M_{1500, \text{AB}} \sim -16$ ) during a star bursts ( $\dot{M}_{\star} \sim 0.04 h^{-1} M_{\odot} \text{ yr}^{-1}$ ) induced by a merger.

The fraction  $\mathcal{R}$  of photons emitted per HI necessary to complete reionization is  $\mathcal{R} = (1 + N_{\text{rec}})/f_{\text{esc}}$ , where  $f_{\text{esc}}$  is the fraction of ionizing photons that can escape their host galaxies and  $N_{\text{rec}}$  is the average number of recombinations per HI. We distinguish between recombinations that occur in (i) mini-haloes, (ii) Lyman-limit systems (LLS), and (iii) in the general intergalactic medium (IGM). Mini-haloes are small high-density clouds that are too cold to form stars via atomic line cooling. The presence of mini-halos can have a significant effect on the propagation and size of HII regions during reionization (Furlanetto & Oh 2005; McQuinn et al. 2007). However, when overrun by an ionization front their gas will be photo-heated and they will eventually evaporate (Shapiro et al. 2004; Iliev et al. 2005b; Ciardi et al. 2006), which decreases their importance in the later stages and after reionization. On the other hand, Lyman-limit systems have sufficiently high column-densities,  $N_{\text{HI}} \gtrsim 10^{17} \text{ cm}^{-2}$ , to self-shield. Ionizing photons impinging on such optically thick systems get converted to (non-ionizing) Lyman- $\alpha$  radiation at high-efficiency (Hogan & Weymann 1987; Rauch et al. 2008). These larger systems determine the mean free path of ionizing photons in the post-reionization era (*e.g.* Miralda-Escude 2003). Below we will concentrate on the third source of recombinations, those occurring in the IGM.

The recombination rate per unit volume,  $\dot{n}_{\text{rec}}$ , depends on the particle density squared,  $\dot{n}_{\text{rec}} = \alpha x^2 n^2$ , where  $x$  is

\* E-mail: milan.raicevic@durham.ac.uk

the mean ionized fraction, and hence varies thorough out the inhomogeneous IGM. Early semi-analytical models of reionization used a mean recombination rate, with the IGM inhomogeneity expressed in terms of a ‘clumping factor’  $\mathcal{C}$ ,  $\langle \dot{n}_{\text{rec}} \rangle = \alpha x^2 \langle n^2 \rangle \equiv \alpha x^2 \mathcal{C} \langle n \rangle^2$  (e.g. Giroux & Shapiro 1996; Tegmark et al. 1997; Ciardi & Ferrara 1997; Haiman & Loeb 1997; Madau et al. 1999; Valageas & Silk 1999). Numerical simulations of Gnedin & Ostriker (1997) yielded high estimates of  $\mathcal{C} \sim 10$  (40) at redshifts  $z = 8$  (5), implying that recombinations are generally quite important. Similar values have been used in the estimate of the comoving star formation rate density needed to keep the post-reionization Universe ionized by balancing ionizations with recombinations. The inferred value,

$$\dot{\rho}_* \approx 0.03 M_{\odot} \text{ yr}^{-1} \text{ Mpc}^{-3} \times \frac{1}{f_{\text{esc}}} \left( \frac{1+z}{8} \right)^3 \left( \frac{\Omega_b h_{70}^2}{0.0457} \right)^2 \left( \frac{\mathcal{C}}{30} \right), \quad (1)$$

(e.g. Madau et al. 1999) is significantly higher at  $z \sim 7$  than some currently observationally inferred rates (e.g. Bunker et al. 2010).

Current numerical simulations model reionization by directly following the propagation of ionization fronts through the inhomogeneous IGM, thus in principle eliminating the need for a clumping factor (e.g. Sokasian et al. 2001; Ciardi et al. 2003; Iliev et al. 2006; McQuinn et al. 2007; Trac & Cen 2007). However the resolution of the radiative transfer (RT) calculation is in general much coarser than that of the density field on which the sources are identified (e.g. Iliev et al. 2010), and a single clumping factor, usually derived from higher resolution small box runs, is used to take account of the density structure below the resolution of the RT mesh (e.g. Ciardi et al. 2003; Iliev et al. 2007).

In this letter we will show that a single value of the clumping factor is, in fact, not appropriate for estimating the recombination rate in numerical RT reionization simulations, and leads to a significant over estimate of the importance of recombinations.

## 2 DEFINITION OF THE CLUMPING FACTOR

The recombination rate of Hydrogen-only gas in a volume  $V$  is

$$\begin{aligned} \dot{N}_{\text{rec}} &= \alpha \int_V n_{\text{H}}^2 dV \\ &\equiv \alpha \mathcal{C} \langle n_{\text{H}} \rangle^2 V, \end{aligned} \quad (2)$$

where  $\alpha$  is the recombination coefficient,  $n_{\text{H}}$  the hydrogen number density,  $\mathcal{C} \equiv \langle n_{\text{H}}^2 \rangle / \langle n_{\text{H}} \rangle^2$  the clumping factor, and we assumed the gas to be fully ionized ( $n_{\text{H}} = n_{\text{HII}}$ ); the angular brackets denote a volume average.

Most current numerical models of reionization follow the formation of dark matter structures in a cosmological setting, compute emissivities of galaxies associated with dark matter halos, then follow how these galaxies ionize their surroundings with a radiative transfer calculation (Ciardi et al. 2003; Iliev et al. 2006; McQuinn et al. 2007; Trac & Cen 2007; Raičević et al. 2010b). Our method in this letter is designed to reproduce the steps taken to set up RT computational meshes in such simulations.

We use a dark matter simulation performed with

the Tree-PM code Gadget-2 (Springel 2005). The simulation uses  $1024^3$  equal-mass particles in a periodic cosmological volume of size  $20 h^{-1}$  comoving Mpc, assuming a flat  $\Lambda$ CDM cosmology with cosmological parameters  $[\Omega_m, \Omega_b, \Omega_{\Lambda}, h, \sigma_8, n_s] = [0.25, 0.045, 0.75, 0.73, 0.9, 1]$ . Baryons are assumed to trace the dark matter, and hence the gas density  $\rho_g$  is related to the matter density  $\rho$  as  $\rho_g = (\Omega_b/\Omega_m)\rho$ . The matter density  $\rho$  at the position  $\mathbf{r}_i$  of particle  $i$  is estimated using the SPH algorithm (Lucy 1977; Gingold & Monaghan 1977),

$$\rho(\mathbf{r}_i) = \sum_j m_j W\left(\frac{|\mathbf{r}_i - \mathbf{r}_j|}{h_i}\right), \quad (3)$$

where  $m_i$  is the particle mass, and  $h_i$  its ‘resolution length’ chosen so that it holds  $\sim 40$  neighboring particles  $j$  that contribute to the sum;  $W$  is the smoothing kernel. The (Hydrogen) number density is computed as  $n_{\text{H}} = (1-Y)\rho_g/m_{\text{p}}$ , where  $Y$  is the primordial Helium abundance by mass, and  $m_{\text{p}}$  is the proton mass.

Assigning a volume  $V_i \approx m_i/\rho_i$  to particle  $i$ , allows us to compute the mean clumping factor as

$$\mathcal{C} = \frac{1}{N_{\text{part}}^2} \sum_i^{N_{\text{part}}} n_{\text{H},i} \sum_i^{N_{\text{part}}} \frac{1}{n_{\text{H},i}}, \quad \text{for } n_{\text{H},i} \leq n_{\text{thr}}, \quad (4)$$

where  $N_{\text{part}}$  is the number of particles in volume  $V$  with number density lower than a given threshold density  $n_{\text{thr}}$ . We use  $n_{\text{thr}} \equiv \Delta_{\text{thr}} \langle n_{\text{H}} \rangle$  with  $\Delta_{\text{thr}} = 100$ , to exclude collapsed halos from the IGM density field (see e.g. Miralda-Escude et al. 2000; Miralda-Escude 2003; Pawlik et al. 2009). Baryons in halos do not trace the dark matter but collapse to form galaxies. Due to their high densities, galaxies should not be treated as general IGM, but rather as LLS and their effect on the propagation of ionizing radiation described in terms of a mean free path, as in e.g. Madau et al. (1997). We chose the overdensity threshold of  $\Delta_{\text{thr}} = 100$  appropriate for the density at the virial radius of a halo, and also to allow for a direct comparison to other works (e.g. Pawlik et al. 2009).

Finally, the RT calculations for large-scale reionization models are usually performed on a uniform cubic mesh, with the density at each mesh point obtained from the  $N$ -body particles using, for example, nearest grid point interpolation (e.g. Hockney & Eastwood 1989). We employ several such grids in the following discussion. The details of the particular simulation we use, and the way we compute densities, are not important as far as our conclusions on recombinations are concerned.

## 3 THE LOCAL CLUMPING

We will make a distinction between two types of clumping factors in the following discussion, both based on Eq. (4). The *global* clumping factor,  $\mathcal{C}_{\text{global}}$ , is computed by summing over *all* particles, as is done in e.g. Iliev et al. (2005a, 2007) and Pawlik et al. (2009). However we can also divide the computational volume in (equal volume, non-overlapping) sub-volumes, *i.e.* a uniform mesh<sup>1</sup>, and evaluate  $\mathcal{C}$  in each

<sup>1</sup> The choice of the volume subdivision is motivated by simplicity. Our conclusions are not dependent on the shape of the mesh

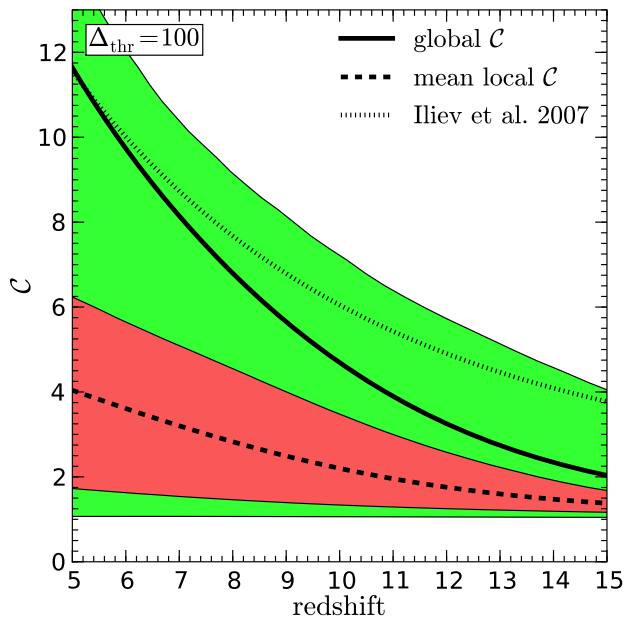


**Figure 1.** Evolution of the clumping factor in a simulation with  $1024^3$  particles in a  $20 h^{-1}$  Mpc box, neglecting particles with overdensities higher than a threshold value of  $\Delta_{\text{thr}} = 100$ . The *black solid line* shows the global clumping factor, which follows reasonably well the result obtained by Iliev et al. (2007; *black dotted line*). We then divide the volume in  $64^3$  equal sub-volumes, and compute the local clumping factor in each of them. The *dashed line* shows the mean local clumping factor, with the 50% (99%) percentiles indicated by the red (green) shaded region. Clearly there is a large scatter in  $C_{\text{local}}$ , and its mean value is significantly lower than that of the global clumping factor.

sub-volume (mesh cell) by summing only over particles in that sub-volume<sup>2</sup>. We will call this a *local* clumping factor,  $C_{\text{local}}$ .

We compare  $C_{\text{global}}$  and  $C_{\text{local}}$  computed on  $64^3$  equal sub-volumes of our  $1024^3$  particles,  $20 h^{-1}$  Mpc aside simulation box in Fig. 1. Our value for  $C_{\text{global}}$  is in reasonable agreement with that obtained by Iliev et al. (2007), even though the relations are derived from significantly different N-body runs. Interestingly however, at any  $z$ , there is a large range of values of  $C_{\text{local}}$ , up to more than a factor of 10 at  $z = 5$ . In addition also the mean value of  $C_{\text{local}}$  in all sub-volumes of the simulation box is significantly lower than that of  $C_{\text{global}}$ . Clearly, a single value of  $C$  is not able to characterize the recombination rate in every region of a simulation.

The mean  $C_{\text{local}}$  in sub-volumes with a given overdensity  $\Delta$  is shown in Fig. 2. This type of  $C(\Delta)$  relation was not previously discussed in the literature. The highest values of  $C_{\text{local}}$  are found in sub-volumes with intermediate overdensity, because clumping is a measure of *inhomogeneity* in the density field. Therefore high clumping is found in sub-volumes that contain high gradients in the density field, for example, small high-density halos in a low density region, or

<sup>2</sup> Note that in general the mean density in each sub-volume will be different as well.

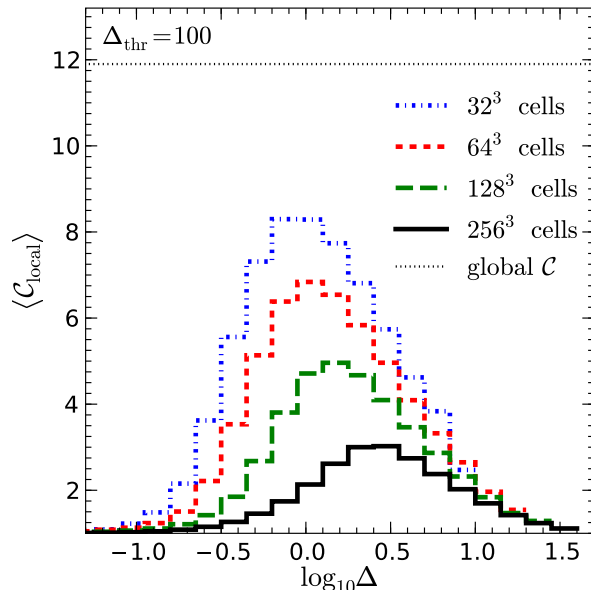


**Figure 2.** Mean local clumping factor ( $\langle C_{\text{local}} \rangle$ ) as a function of the overdensity ( $\Delta$ ) of the sub-volume, at redshift  $z = 5$ , for various subdivisions of the computational volume; the corresponding cell sizes are  $625$ ,  $312.5$ ,  $156.25$  and  $78.125 h^{-1}$  kpc. Coarser sub-cells yield higher values of  $\langle C_{\text{local}} \rangle$  at a given overdensity, and  $\langle C_{\text{local}} \rangle$  peaks at intermediate values of the overdensity. The value of  $C_{\text{global}}$  is shown as a black dotted line.

the transition between a filament and a void. Improving the sampling of the density field by using smaller sub-volumes, decreases the peak amplitude in  $C_{\text{local}}$ , and moves the maximum toward higher overdensity regions, but does not change the general shape of the distribution. The general shape is also not strongly affected by the choice of  $\Delta_{\text{thr}}$ . Note that the recombination rate, which is  $\propto C_{\text{local}} \Delta^2$ , is still highest in the highest density regions. However, the use of  $C_{\text{local}}$  distribution shown in Fig. 2 increases the relative contribution of moderately overdense regions to the total recombination rate.

An inaccurate estimate of the clumping factor of course also implies that the recombination rate is not accurate, and hence that the speed of ionisation fronts are not computed correctly. Instead of studying the effects on a full RT reionization run, we show a simpler example by calculating recombination rates in the  $20 h^{-1}$  Mpc,  $1024^3$  particles simulation box at redshift  $z = 5$ , including densities up to a threshold of  $\Delta_{\text{thr}} = 100$  and assuming that all gas is fully ionised. We can sum the recombination rate per particle,  $\dot{N}_{\text{rec},i} = \alpha (m/m_p^2) \rho_{g,i}$ , over all particles  $i$ , to get the total recombination rate,  $\dot{N}_{\text{rec,correct}} = \sum \dot{N}_{\text{rec},i}$ . This is the ‘correct’ recombination rate as it takes into account all the available density field information from the N-body simulation. We compare the value of  $\dot{N}_{\text{rec,correct}}$  to values obtained by first interpolating particle densities to a mesh as described in Section 2, and computing the sum of  $\dot{N}_{\text{rec}}$  in each mesh cell using different expressions for the clumping factor (Fig. 3). Not using a clumping factor (yellow bars) shows the effect of the density field smoothing by the mesh as the recombination rates are both underestimated (a factor of two even

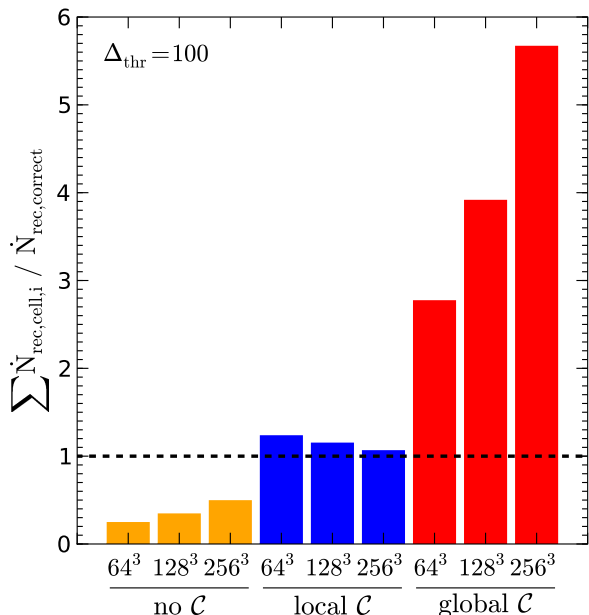


**Figure 3.** Recombination rate,  $\dot{N}_{\text{rec}}$ , in a fully-ionized simulation box of  $20 h^{-1}\text{Mpc}$  at redshift  $z = 5$  when simulated using  $1024^3$  particles, assuming gas traces dark matter, and imposing an overdensity threshold of  $\Delta_{\text{thr}} = 100$ . The recombination rate is computed using various sizes of the sub-volumes over which to compute the clumping factor, and is expressed in units of the ‘correct’ value computed directly from the  $N$ -body particles. Not using a clumping factor at all ( $\mathcal{C} = 1$ ; yellow bars) leads to an underestimate of  $\dot{N}_{\text{rec}}$ , which get less at improved sub-sampling of the density field. Using a global value ( $\mathcal{C}_{\text{global}}$ ; red bars) leads to a large overestimate of  $\dot{N}_{\text{rec}}$ , which gets *worse* at improved sampling. Finally using a locally estimated clumping factor ( $\mathcal{C}_{\text{local}}$ ; blue bars) gives a much more accurate value of  $\dot{N}_{\text{rec}}$ , which is also nearly independent of the sampling resolution.

at the highest grid resolution) and strongly mesh resolution dependent. On the other hand, when the global clumping  $\mathcal{C}_{\text{global}}$  is used to represent the sub-grid matter distribution (red bars), it significantly overestimates the recombination rate while not remedying the dependence on mesh resolution. This is no surprise as a single value of clumping simply linearly increases the no clumping result. Crucially, using the locally estimated clumping factor,  $\mathcal{C}_{\text{local}}$  (blue bars), leads to a much more accurate and resolution independent description of recombinations (within  $\sim 25\%$  of  $\dot{N}_{\text{rec,correct}}$  on all grid resolutions). Note that the assumption of a fully ionized simulation box is a special case, chosen for illustrative purposes. A more relevant case for the study of reionization is a partially ionized cosmological density field. The most important consequence of using  $\mathcal{C}_{\text{local}}$  instead of  $\mathcal{C}_{\text{global}}$  is a much lower average recombination rate, for whichever overdensity regions are ionized at any time. The convergence of recombination rates obtained in Fig. 3 with the use of  $\mathcal{C}_{\text{local}}$  also leads to the convergence of I-front speeds during reionization as we will show in Raičević et al. (2010b), where we also discuss the ionized fraction as a function of overdensity during reionization. Also,  $\mathcal{C}_{\text{local}}$  is computed assuming a full ionization and does not provide a perfectly accurate recombination rate estimate for partially ionized sub-volumes. Therefore, the use of a higher resolution RT computational

mesh is always preferable to employing any kind of clumping.

## 4 CONCLUSIONS

Clumping factors are often used in simulations of reionization to represent the unresolved matter inhomogeneity, below the computational mesh resolution, which may significantly contribute to the recombination rates (e.g. Ciardi et al. 2003; Iliev et al. 2007; McQuinn et al. 2007). Here we have shown that, because the density field during reionization is so inhomogeneous, using a single clumping factor in general leads to a significant over estimate of the recombination rate (factors of several), which may in fact get worse as the grid resolution is improved. As a consequence the speed of ionization fronts is artificially depressed, reionization delayed, and the outcome of the radiative transfer simulations significantly resolution dependent.

McQuinn et al. (2007) improved on this issue by analytically deriving the clumping factor as a function of overdensity,  $\mathcal{C} = \mathcal{C}(\Delta)$ , and also Kohler et al. (2007) took into account some density dependence by splitting their simulation volumes into 8 equal sub-volumes. However, both ignored the fact that clumping still depends on the volume over which it is computed (i.e. the size of the sub-volumes), and that dependence is not negligible as shown in Fig. 2. Not taking the volume into account will always lead to the RT results depending on the computational mesh resolution.

Fortunately it is not computationally intensive to compute a local clumping factor on a reasonably fine grid. The recombination rate obtained using this clumping factor is very close to the ‘correct’ value inferred directly from the particles themselves, and is not very sensitive to the resolution of the mesh used (see Fig. 3). In our dark matter only simulations the cell size should be such that most of the structures are resolved, and should ideally be close to the Jeans mass of the photo-ionised IGM (Pawlik et al. 2009). We therefore argue that any future fits of clumping factors aimed for use in RT simulations of reionization must include both density and volume dependence. The alternative of computing the recombination rate per particle directly (Trac & Cen 2007), is far more computationally expensive.

## ACKNOWLEDGMENTS

MR would like to thank Garrelt Mellema and Joop Schaye for useful discussions. During the work on this paper, MR was supported by a grant from Microsoft Research Cambridge.

## REFERENCES

- Arons J., Wingert D. W., 1972, ApJ, 177, 1
- Barkana R., Loeb A., 2001, Physics Reports, 349, 125
- Bouwens R. J., Illingworth G. D., Franx M., Ford H., 2008, ApJ, 686, 230
- Bouwens R. J., et al. 2009, arXiv:0912.4263
- Bunker A. J., et al. 2010, MNRAS, pp 1378
- Ciardi B., Ferrara A., 1997, ApJ, 483, L5
- Ciardi B., Ferrara A., 2005, SSR, 116, 625

- Ciardi B., Scannapieco E., Stoehr F., Ferrara A., Iliev I. T., Shapiro P. R., 2006, MNRAS, 366, 689
- Ciardi B., Stoehr F., White S. D. M., 2003, MNRAS, 343, 1101
- Furlanetto S. R., Oh S. P., 2005, MNRAS, 363, 1031
- Gingold R. A., Monaghan J. J., 1977, MNRAS, 181, 375
- Giroux M. L., Shapiro P. R., 1996, ApJS, 102, 191
- Gnedin N. Y., Ostriker J. P., 1997, ApJ, 486, 581
- Gunn J. E., Peterson B. A., 1965, ApJ, 142, 1633
- Haardt F., Madau P., 1996, ApJ, 461, 20
- Haiman Z., Loeb A., 1997, ApJ, 483, 21
- Hockney R. W., Eastwood J. W., 1989, Computer simulation using particles. Taylor & Francis, 1989
- Hogan C. J., Weymann R. J., 1987, MNRAS, 225, 1
- Iliev I. T., Ahn K., Koda J., Shapiro P. R., Pen U., 2010, arXiv:1005.2502
- Iliev I. T., Mellema G., Pen U., Merz H., Shapiro P. R., Alvarez M. A., 2006, MNRAS, 369, 1625
- Iliev I. T., Mellema G., Shapiro P. R., Pen U., 2007, MNRAS, 376, 534
- Iliev I. T., Scannapieco E., Shapiro P. R., 2005a, ApJ, 624, 491
- Iliev I. T., Shapiro P. R., Raga A. C., 2005b, MNRAS, 361, 405
- Kohler K., Gnedin N. Y., Hamilton A. J. S., 2007, ApJ, 657, 15
- Komatsu E., et al. 2010, arXiv:1001.4538
- Loeb A., 2006, arXiv:astro-ph/0603360
- Lucy L. B., 1977, AJ, 82, 1013
- Madau P., Haardt F., Rees M. J., 1999, ApJ, 514, 648
- Madau P., Meiksin A., Rees M. J., 1997, ApJ, 475, 429
- McQuinn M., Lidz A., Zahn O., Dutta S., Hernquist L., Zaldarriaga M., 2007, MNRAS, 377, 1043
- Miralda-Escude J., 2003, ApJ, 597, 66
- Miralda-Escude J., Haehnelt M., Rees M. J., 2000, ApJ, 530, 1
- Pawlik A. H., Schaye J., van Scherpenzeel E., 2009, MNRAS, 394, 1812
- Raičević M., Theuns T., Lacey C., 2010a, arXiv:1008.1785
- Raičević M., Theuns T., Lacey C., Paardekooper J.-P., 2010b, in preparation
- Rauch M., 1998, ARA&A, 36, 267
- Rauch M., et al. 2008, ApJ, 681, 856
- Shapiro P. R., Iliev I. T., Raga A. C., 2004, MNRAS, 348, 753
- Sokasian A., Abel T., Hernquist L. E., 2001, New Astronomy, 6, 359
- Springel V., 2005, MNRAS, 364, 1105
- Tegmark M., Silk J., Rees M. J., Blanchard A., Abel T., Palla F., 1997, ApJ, 474, 1
- Trac H., Cen R., 2007, ApJ, 671, 1
- Valageas P., Silk J., 1999, A&A, 347, 1